Eur. Phys. J. E (2012) **35**: 129
DOI 10.1140/epje/i2012-12129-3

THE EUROPEAN PHYSICAL JOURNAL E

Regular Article

Competition between substrate-mediated π-π stacking and surface-mediated T_g depression in ultrathin conjugated polymer films

Tao Wang[1,a], Andrew J. Pearson[1], Alan D.F. Dunbar[2], Paul A. Staniec[3], Darren C. Watters[1], David Coles[1], Hunan Yi[4], Ahmed Iraqi[4], David G. Lidzey[1], and Richard A.L. Jones[1]

[1] Department of Physics and Astronomy, University of Sheffield, Sheffield, S3 7RH, UK
[2] Department of Chemical and Biological Engineering, University of Sheffield, Sheffield, S1 3JD, UK
[3] Diamond Light Source Ltd, Diamond House, Harwell Science and Innovation Campus, Didcot, Oxfordshire, OX11 0DE, UK
[4] Department of Chemistry, University of Sheffield, Sheffield, S3 7HF, UK

Received 4 July 2012 and Received in final form 5 October 2012
Published online: 14 December 2012

Abstract. We report surface and interface effects in dynamics and chain conformation in the thin film of conjugated polymer PCDTBT. To probe dynamic anomalies, we measure the glass transition temperature (T_g) of PCDTBT films as a function of thickness, and find that there is a significant depression in T_g for films less than 100 nm thick; a result qualitatively similar to that observed in many other polymer film systems. However, for films less than 40 nm, the T_g converges to a constant value of 20 K below its bulk value. Grazing incidence X-ray diffraction shows depth-dependent molecular organization that is associated with the unusual thickness-dependent dynamics.

1 Introduction

Polymers have demonstrated deviations from their bulk physical properties when they are in confinement [1–4]. Such phenomena are very striking in thin polymer films, for which the glass transition temperature (T_g) [1–4] and viscosity [5,6] are widely observed to deviate significantly from bulk values when a film is created having a thickness below some critical value. Whilst the enhanced dynamics of polymer chains at a free surface will always reduce T_g [7], strong polymer-substrate interactions can often increase T_g [1,8]. Such effects can be quantified using models [1,9,10] that describe a thin-film consisting of a number of separate layers in which the polymer molecules have different chain mobility. Despite this growing understanding of the structure of thin films of saturated polymers, less is known regarding the deviation of bulk properties of conjugated polymers when they are formed into thin films, although one study has observed a deviation in T_g in two fluorene-based conjugated polymers [11]. Conjugated polymers usually have greater chain stiffness than conventional saturated polymers (for example polystyrene) that has served as a model system to study T_g deviation in thin films. Although some conjugated polymers are non-crystalline, an intermediate level of order is usually present resulting from π-π stacking between polymer backbones. Despite the importance of this class of device applicable material, the effect of a substrate or an interface on such states of intermediate order is not however well understood.

In this work, we explore the changes in T_g and molecular organization of thin films of a conjugated polymer poly[N-9′-heptadecanyl-2,7-carbazole-alt-5,5-(4′, 7′-di-2-thienyl-2′, 1′, 3′-benzothiadiazole)] (PCDTBT). PCDTBT is one of a relatively new class of low-energy-gap polymers that have been used to fabricate photovoltaic devices and field effect transistors [12,13]. Our measurements suggest the existence of a series of distinct depth-dependent morphological phases within the film, with a π-π stacked layer having increased coherence length existing close to the substrate and lamellar-type order towards the film surface. We speculate that such structural heterogeneity may directly affect the electronic properties of conjugated polymer thin films; a conclusion that has relevance for the operation of organic-electronic devices [14,15].

2 Experimental methods

The polymer PCDTBT was synthesized according to our previous report [16], and had an M_w of 29.3 kDa and a polydispersity of 1.57 as measured by GPC. Figure 1

[a] e-mail: t.wang@hotmail.com

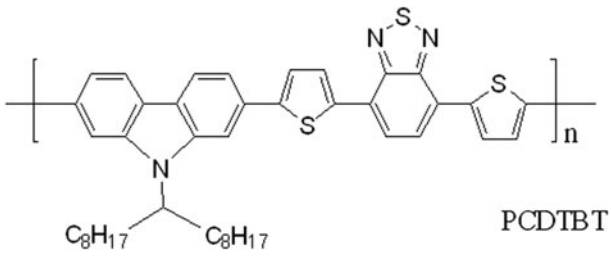

Fig. 1. The molecular structure of PCDTBT.

shows the molecular structure of PCDTBT. GPC was performed in 1,2,4-trichlorobenzene (TCB) at a temperature of 100 °C. The GPC curves were obtained by the RI-detection method, with a series of narrow polystyrene standards used to calibrate the instrument. To prepare thin films, PCDTBT was dissolved in chlorobenzene (CB) at a range of different concentrations (from 1.3 to 40 mg/ml) and deposited on a Si/SiO_x substrate by spin-casting to create films having thickness between 12 and 200 nm. In each case a fixed spin speed was used (1000 rpm) to reduce the varying effects of the centrifugal force on intermolecular interactions during spin casting. Spectroscopic ellipsometry was used to determine film thickness, with a Cauchy model used to fit Ψ and Δ over the wavelength range in which the film is optically transparent.

To determine T_g, PCDTBT films were heated from 25 to 200 °C under a N_2 atmosphere and then cooled to 25 °C at a rate of 2 °C/min. The thickness-dependent T_g of PCDTBT films was measured using ellipsometry during a cooling cycle. Grazing-incidence wide-angle X-ray scattering (GIWAXS) measurements were carried at the I-16 beamline, Diamond Light Source (UK). Samples were mounted in a custom-built experimental chamber (filled with helium to reduce scatter) featuring an internal beamstop and blade held above the sample as described previously [13]. PCDTBT samples for GIWAXS measurement were either studied as-cast, or were annealed *ex situ* by heating to 200 °C and then returned to room temperature at a rate of 2 °C/min. This process replicates the thermal protocol used to study films using ellipsometry to determine the T_g. All films were prepared on clean Si/SiO_x wafers. A series of GIWAXS scattering patterns were recorded at different grazing incidence angles with a step of 0.02°, using 12 keV energy X-rays and a Pilatus 2M detector to record images with a 30 second exposure time.

3 Results and discussion

Our previous work has demonstrated that any residual CB casting solvent trapped in a PCDTBT film during spin-casting evaporates rapidly during the initial heating cycle once the film reaches a temperature of 135 °C (the boiling point of CB) [13]. This process removes all casting solvent from the film, and thus on cooling we can use the change in the gradient of Ψ to extract the T_g. We have confidence in this procedure, as the coincidence and reproducibility of the change in Ψ as a function of temperature observed on the first cooling cycle and second heating cycle are excellent. We do not expect degradation of PCDTBT to occur in our measurements as all heating/cooling cycles were performed under a N_2 atmosphere at temperatures well below the degradation temperature [17] of PCDTBT (> 450 °C).

Figure 2a summarizes recorded values of Ψ (at 650 nm) determined using ellipsometry for films having different thickness as a function of temperature. Interestingly as the film thickness is reduced below 40 nm, the difference in the slope of the glassy and rubbery regime reduces, indicative of a reduced strength of the T_g transition in such thin films. This behavior is qualitatively similar with that observed in saturated PS films [18]. It is also notable that the width of the T_g transition apparently reduces as the T_g of PCDTBT thin film is reduced; a conclusion evidenced from the temperatures at which the expansion of the film (as measured by Ψ at 650 nm) deviates from linearity.

Figure 2b shows that as the PCDTBT film thickness reduces, T_g is reduced from 130 °C at 100 nm to around 110 °C at 40 nm. This relatively small depression in T_g (20 °C) is smaller than that has been observed in polystyrene, where a T_g reduction up to 40 °C has been observed [1]. Interestingly, the depression in T_g in PS only occurs when the film thickness is less than 50 nm [1], whilst in PCDTBT this effect occurs once the film is reduced below 100 nm; a result in accord with another study on two fluorene-based conjugated polymers [11]. The most striking feature presented in fig. 2b is that the T_g of the PCDTBT film converges to a value of approximately 110 °C (*vide infra*) at a film thickness of 40 nm and does not undergo additional reduction as the film is further thinned, whereas in PS films the T_g continues to decrease even when the film thickness is reduced below 40 nm.

We can understand the differences between the onset thickness of T_g depression in PCDTBT and PS on the basis of chain stiffness; previous work [19] on polycarbonate (having a chain stiffness greater than PS) has found the onset thickness for T_g deviation starts at 142 nm, a value much larger than the critical thickness of PS. Ellison *et al.* [20] also found that modification of the PS monomer unit can substantially change the T_g deviation behavior, and concluded that chain stiffness is responsible for increased onset thickness of the depressed-T_g surface layer via its influence on the cooperative segmental size of the polymers. We conclude therefore that PCDTBT has a higher chain stiffness than PS, resulting in a comparatively larger cooperative segmental size and a higher onset thickness for T_g deviation.

We can quantify the T_g depression behavior in films having a thickness between 100 and 40 nm using a phenomenological two-layer model [1] as expressed using eq. (1). Here the parameter γ empirically describes the thickness of the surface layer with δ being a fitting constant and h the entire thickness of the film,

$$T_g = T_g^{\text{bulk}} \left[1 - \left(\frac{\gamma}{h}\right)^{\delta}\right]. \quad (1)$$

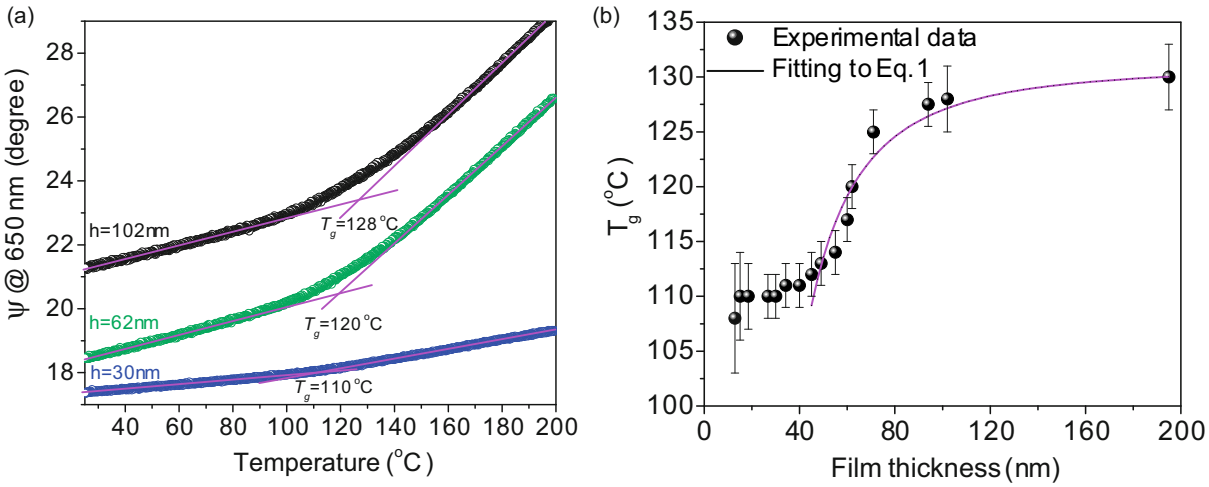

Fig. 2. Anomalous glass transition temperatures in PCDTBT thin films. (a) T_g of PCDTBT films having different thickness as determined during cooling by ellipsometry. (b) T_g as a function of film thickness. The solid line is a best fit to the T_g depression region (40–100 nm) using eq. (1).

We find that this model provides a good fit to the experimental data within the T_g depression region. From our best fit ($\chi^2 = 4.6$), we obtain the bulk values $T_g^{\text{bulk}} = 131\,^{\circ}\text{C}$, $\gamma = 19.3\,\text{nm}$ and $\delta = 2.1$. The value of T_g^{bulk} determined here agrees well with a previous measurement of the bulk T_g of PCDTBT of 130 °C determined using differential scanning calorimetry [17].

In direct contrast to polymers having a saturated molecular backbone, PCDTBT molecules undergo π-π stacking in a solid thin film after spin casting from solution. We have used grazing-incidence wide-angle X-ray scattering (GIWAXS) to study the π-π stacking in PCDTBT following our previously reported methodology [13]. The data shown in fig. 3a was recorded from an as-cast (unannealed) PCDTBT film. Here, π-π stacking is evidenced via a scattering "crescent" observed at $q = 1.57\,\text{Å}^{-1}$ in the 2D X-ray scattering image [13,21]. The fact that this peak is primarily in the out-of-plane direction indicates that the conjugated backbones adopt a face-on orientation and lay parallel to the silicon substrate. The innermost diffraction ring at a $q = 0.31\,\text{Å}^{-1}$ (partly blocked in the out-of-plane direction by the flare after the beam stop) is attributed to 1st-order scattering from side-chain ordering, and is associated with the distance (ca. 20 Å) between bi-layer ordered lamella of PCDTBT backbones separated by the two alkyl side-chain lengths [13, 21,22].

The data presented in fig. 3b was recorded from a PCDTBT film that had been subject to the same heating and cooling cycles used in the ellipsometry measurements used to determine T_g. Here, a new diffraction peak at $q = 0.63\,\text{Å}^{-1}$ appears in the out-of-plane direction of the 2D image: a feature recently assigned as the 2nd-order diffraction of the bi-layer lamella spacing [22]. Such a structure is observed if a PCDTBT film is annealed above its bulk T_g and originates from PCDTBT molecules adopting a lamellar structure with an edge-on orientation [22]. Our X-ray scattering measurements presented here confirm therefore that the molecular structure in PCDTBT films upon thermal treatment above the bulk T_g is characterized by an admixture of face-on stacking and edge-on lamellar stacking.

We have used GIWAXS measurements performed as a function of grazing-incidence angle (α) to probe the structure as a function of depth below the film surface [23]. This permits us to determine π-π stacking coherence length using $L = 2\pi/\Delta q$, where Δq is the full width at half-maximum of the scattering crescent observed at $q = 1.57\,\text{Å}^{-1}$. Here, Δq is determined from a Gaussian multi-peak fit to the raw scattering data in the out-of-plane direction, a selection of which is shown in fig. 3c. We summarize the π-π stacking coherence length determined at different incidence angles in fig. 3d, with data plotted for two films having a thickness of 30 and 50 nm. In the same plot, we also show the ratio of the scattering intensity ($I_{q1.57}/I_{q0.63}$) of the scattering features at $q = 1.57\,\text{Å}^{-1}$ (π-π stacking) and $q = 0.63\,\text{Å}^{-1}$ (lamella packing), again as a function of X-ray incidence angle.

To understand the significance of such data, it is necessary to relate grazing-incidence angles (α) to the regions in the film at which X-ray scattering is being generated. For grazing-incidence angles less than the critical angle for total reflection from the polymer (α_c^{pol}), we can straightforwardly calculate the penetration depth of the X-rays at grazing-incidence angles $\alpha < \alpha_c^{\text{pol}}$ using the methodology outlined in Appendix A. Here, the X-ray scattering process is confined to a depth $< 15\,\text{nm}$ from the surface. We find that close to the film surface ($\alpha = 0.03°$) the π-π stacking coherence length is approximately (7.0 ± 0.5) Å (see fig. 3d). For incidence angles $\alpha_c^{\text{pol}} < \alpha < \alpha_c^{\text{Si}}$ (where α_c^{Si} is the critical angle of the Si substrate), a standing wave forms in the film as a result of interference between the incident X-ray beam and the beam reflected from the polymer-substrate interface [24]. We calculate the structure of this standing wave as outlined in Appendix A (and shown in figs. 4 and 5). For this range of angles,

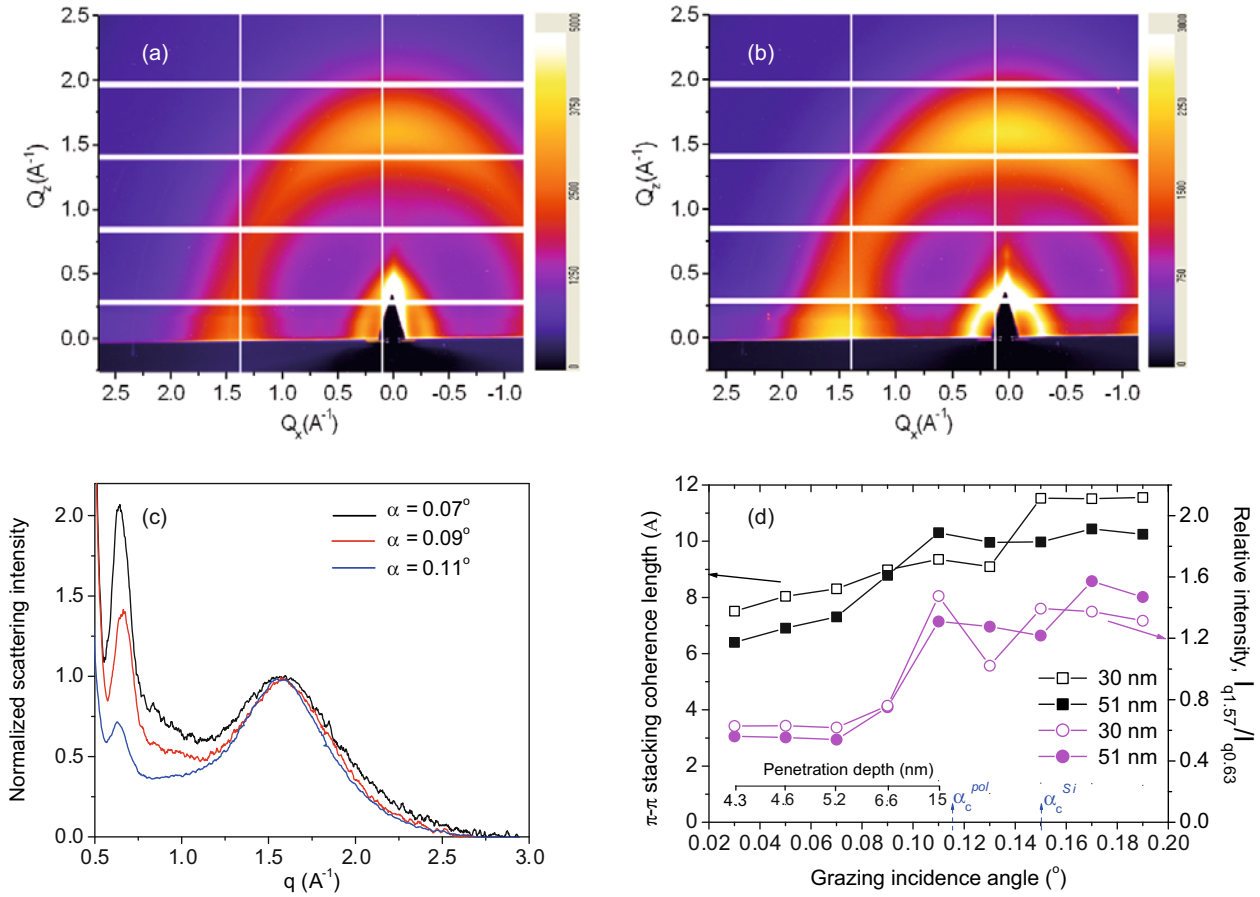

Fig. 3. Heterogeneous vertical structure in PCDTBT thin films. 2D grazing incidence X-ray images of a 50 nm thick film at $\alpha = 0.11°$ in an as-cast state (a) and after the heating/cooling cycle for T_g measurement (b). Panel (c) shows the raw scattering data for a 50 nm thick film at three different grazing incidence angles in the out-of-plane direction. Panel (d) shows the π-π stacking coherence length as a function of grazing incidence angle, together with the relative intensity changes of peaks at $q = 0.63$ and $1.57\,\text{Å}^{-1}$.

the scattering signal reflects some weighted average of molecular structure throughout the depth of the film. For $\alpha > \alpha_c^{\text{Si}}$, the X-ray beam penetrates the entire depth of the PCDTBT film and also enters the Si/SiO_x substrate. Here, the X-rays probe the average structure throughout the entire depth of the film, with the π-π stacking coherence length being (11.0 ± 0.5) Å.

The data presented in fig. 3d suggest that π-π stacking is more pronounced towards the underlying interface, indicating that intermolecular π-π stacking is stabilized by the silicon substrate. In figs. 3c and d it is also apparent that the intensity of the 2nd-order lamellar spacing diffraction peak at $q = 0.63\,\text{Å}^{-1}$ becomes relatively stronger at smaller X-ray incidence angles, indicating that lamella stacking is more pronounced towards the film surface. Previous X-ray studies [13,21] have demonstrated that π-π stacking is disrupted (as evidenced by its reduced coherence length) in a PCDTBT film that has been previously thermally annealed. As π-π stacking results in the strongest possible intermolecular interaction between PCDTBT molecules, we conclude that reduced π-π stacking in a PCDTBT film will lead to a decreased T_g. Indeed, using spectroscopic ellipsometry we have found that the T_g of a PCDTBT film is more than 10 °C higher on its 1st heating cycle compared to its first cooling cycle [13]. During the 1st heating cycle, the T_g measurement probes a film in an as-cast state with π-π stacking representing the dominant state of molecular order. However during the 1st cooling cycle, the mixture of molecular arrangements that are generated by the initial heating cycle (π-π stacking and lamellar order) determine the average T_g of the film. Our results suggest therefore that molecules that undergo lamella packing are characterized by a reduced level of π-π stacking, which results in a depressed T_g at the free-surface region of a PCDTBT thin film. In contrast, the stabilized π-π stacking that occurs at the silicon substrate interface is likely to restrict chain mobility and —we concluded— increases the local T_g around this interface. Figure 3d suggests that in a thick PCDTBT film, the surface layer with a depressed T_g should be less than 15 nm, since the π-π stacking coherence length and relative intensity of $I_{q1.57}/I_{q0.63}$ begin to saturate at ≥ 15 nm below the film surface.

We speculate therefore that an annealed PCDTBT film is essentially composed of three distinct layers; a surface layer dominated by lamella ordering which has

reduced π-π stacking, a bulk intermediate layer and an interface layer with pronounced π-π stacking that is stabilized by interaction with the substrate. As the film is progressively thinned, a reduction occurs in the thickness of the bulk layer. As the total film thickness falls below 40 nm, this bulk layer vanishes entirely, resulting in a film consisting of a lamellar-ordered surface-layer positioned on a substrate layer having pronounced π-π stacking. Here, a competition arises between the substrate-directed π-π stacked layer (having increased T_g) and a lamella-ordered layer located at the film surface having reduced π-π stacking and thus depressed T_g. This results in the apparent convergence of T_g to 110 °C even in the thinnest films studied. Without the existence of the π-π stacking driven by the presence of the substrate interface, we anticipate that the T_g would not converge as observed but would undergo further reduction as the film is thinned. Indeed, the ellipsometry data presented in fig. 2a suggests that the width of the T_g transition reduces as the total thickness of the PCDTBT film is reduced, an observation consistent with a relative increase in the volume fraction of the π-π stacked layer and a general reduction in conformational heterogeneity.

We believe the observation of the heterogeneous molecular structure in conjugated-polymer thin films has significant relevance for their application in organic electronic devices. It is known that coherence length in a conjugated polymer phase can substantially increase the efficiency of bulk heterojunction solar cells [25]. However, our measurements demonstrate a variation in coherence length that is driven by proximity to an interface and a free surface. This effect will be particularly important in devices such as bottom-gate field effect transistors (FET) that utilize a SiO_2 gate dielectric. Here, charge transport occurs through a channel having a width of a few nanometers positioned in close proximity to the gate insulator. π-π stacking in this layer driven by interactions with the substrate will be particularly important in generating a molecular system having high charge-carrier mobility. Clearly, the degree of π-π stacking driven by interactions with the substrate will be dependent on the nature of the substrate, and on the propensity of the (macro)-molecules under study to undergo π-π stacking. Nevertheless the ability to control and drive this process has wider important implications for the efficient operation of organic-based light-emitting diodes or photovoltaic devices, as molecular-scale order is likely to increase charge-carrier mobility and thus increase the rate at which charges can be injected or extracted. Developing methods to control nanoscale order close to an interface by —for example— controlling surface energy may present a useful means to optimize such electronic properties.

4 Conclusions

In conclusion, we have quantified depth-dependent morphological structure within a PCDTBT conjugated-polymer thin film using spectroscopic ellipsometry and grazing-incidence X-ray scattering. Our results indicate a thickness-dependent glass transition temperature that results from a competition between π-π stacking driven by proximity to the substrate and lamellar structure with reduced π-π stacking near the film's free surface. Our work provides insight into heterogeneity in molecular morphology and in particular provides a methodology to explore the effect of different device-applicable substrate materials and interfaces on controlling electronic functionality.

We thank the UK EPSRC for funding this work under grant EP/F0164331 and EP/I028641/1. We thank Diamond Light Source via a program grant MT1203 for the X-ray scattering experiment.

Appendix A. X-ray penetration depth at different grazing-incidence angle

X-ray electric-field depth intensity

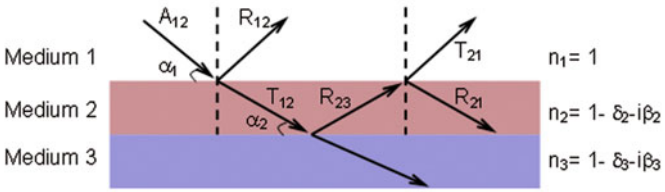

Fig. 4. The incidence (A), reflection (B) and transmission (T) of X-ray in a three-layer system. The refractive index n of an electromagnetic medium for X-ray is $n = 1 - \delta - i\beta$, with δ the refractive index decrement and β the absorption index. The real and complex parts of the refractive index are assumed to be constant throughout the film. Both medium 1 (air) and substrate are considered infinite and lossless media. At 12 keV, the refractive index of the polymer layer is $n = 1\text{–}2.0 \times 10^{-6} - i(2.0 \times 10^{-9})$, and $n = 1\text{–}3.36 \times 10^{-6} - i(4.4 \times 10^{-8})$ for Si.

When the grazing-incidence angle of the X-ray beam is below the critical angle (α_c) of the thin film, the electric field intensity in the film is evanescent in nature and decays exponentially as a function of depth. For angles $\alpha < \alpha_c$ we can quantify the penetration depth (l) of the X-rays into the film using eq. (A.1) [26,27].

$$l = \frac{\sqrt{2}\lambda}{4\pi}\sqrt{\left[\left(\alpha^2 - \alpha_c^2\right)^2 + \left(\lambda\mu_m\rho/4\pi\right)^2\right]^{-1/2} + \alpha_c^2 + \alpha^2}. \tag{A.1}$$

Here, λ is the wavelength of synchrotron X-ray, μ_m is the mass absorption coefficient of the film and ρ its density, assumed to be 1300 kg m^{-3}, $\alpha_c = 0.115°$. The critical angle is calculated using $\alpha_c = \sqrt{\frac{2\lambda^2 r_e N_A Z_\rho}{2\pi A}}$, where λ is the wavelength of the incident X-rays (1.033 Å), r_e is the classical electron radius (2.814×10^{-14} nm), N_A is Avogadro's number, Z the averaged atomic number and A the averaged atomic mass. For incidence angles between the

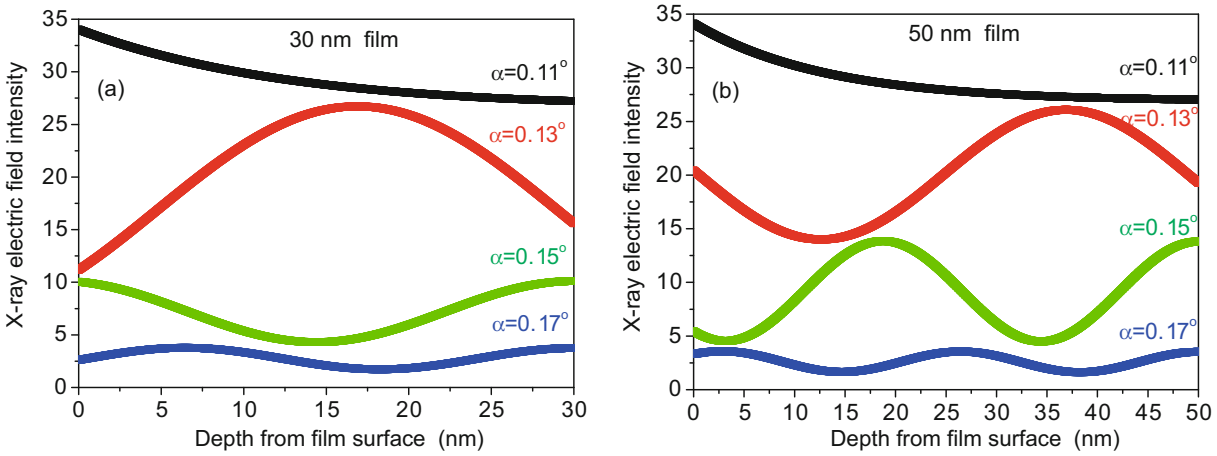

Fig. 5. X-ray electric-field intensity as a function of depth at different incidence angles in films with a thickness of (a) 30 nm and (b) 50 nm. The curves are offset for clarity.

critical angle of the polymer (α_c^{pol}) and the Si substrate ($\alpha_c^{\mathrm{Si}} = 0.15°$ for 12 keV X-rays) the X-ray beam penetrates into the bulk of the film, with a standing wave being formed as a result of interference between the incident beam and the beam reflected from the polymer-substrate interface [24]. The calculation of the electromagnetic field intensity distribution as a function of depth using a transfer matrix reflectivity model [28] indicates that the field maximum of the standing wave locates close to the centre of the film (for a 30 nm thick film) or near the interface with the Si substrate (for a 50 nm thick film) (see fig. 5). For $\alpha > \alpha_c^{\mathrm{Si}}$, the X-ray beam penetrates the entire depth of the PCDTBT film and enters the Si/SiO_x substrate, probing an averaged structure of the whole film.

References

1. J.L. Keddie, R.A.L. Jones, R.A. Cory, Europhys. Lett. **27**, 59 (1994).
2. J.A. Forrest, K. Dalnoki-Veress, J.R. Stevens, J.R. Dutcher, Phys. Rev. Lett. **77**, 2002 (1996).
3. G.B. DeMaggio, W.E. Frieze, D.W. Gidley, M. Zhu, H.A. Hristov, A.F. Yee, Phys. Rev. Lett. **78**, 1524 (1997).
4. C.J. Ellison, J.M. Torkelson, Nat. Mater. **2**, 695 (2003).
5. Z.H. Yang, Y. Fujii, F.K. Lee, C.H. Lam, O.K.C. Tsui, Science **328**, 1676 (2010).
6. H. Bodiguel, C. Fretigny, Phys. Rev. Lett. **97**, 266105 (2006).
7. Z. Fakhraai, J.A. Forrest, Science **319**, 600 (2008).
8. D.S. Fryer, R.D. Peters, E.J. Kim, J.E. Tomaszewski, J.J. de Pablo, P.F. Nealey, C.C. White, W.L. Wu, Macromolecules **34**, 5627 (2001).
9. J.A. Forrest, J. Mattsson, Phys. Rev. E **61**, 53 (2000).
10. J.H. Kim, J. Jang, W.C. Zin, Langmuir **17**, 2703 (2001).
11. M. Campoy-Quiles, M. Sims, P.G. Etchegoin, D.D.C. Bradley, Macromolecules **39**, 7673 (2006).
12. S. Cho, J.H. Seo, S.H. Park, S. Beaupre, M. Leclerc, A.J. Heeger, Adv. Mater. **22**, 1253 (2010).
13. T. Wang, A.J. Pearson, A.D.F. Dunbar, P.A. Staniec, D.C. Watters, H. Yi, A.J. Ryan, R.A.L. Jones, A. Iraqi, D.G. Lidzey, Adv. Funct. Mater. **22**, 1399 (2012).
14. C. Kim, A. Facchetti, T.J. Marks, Science **318**, 76 (2007).
15. C. Kim, A. Facchetti, T.J. Marks, J. Am. Chem. Soc. **131**, 9122 (2009).
16. H. Yi, S. Al-Faifi, A. Iraqi, D.C. Watters, J. Kingsley, D.G. Lidzey, J. Mater. Chem. **21**, 13649 (2011).
17. N. Blouin, A. Michaud, D. Gendron, S. Wakim, E. Blair, R. Neagu-Plesu, M. Belletête, G. Durocher, Y. Tao, M. Leclerc, J. Am. Chem. Soc. **130**, 732 (2008).
18. S. Kawana, R.A.L. Jones, Phys. Rev. E **63**, 021501 (2001).
19. C.L. Soles, J.F. Douglas, W. Wu, H. Peng, D.W. Gidley, Macromolecules **37**, 2890 (2004).
20. C.J. Ellison, M.K. Mundra, J.M. Torkelson, Macromolecules **38**, 1767 (2005).
21. Z.M. Beiley, E.T. Hoke, R. Noriega, J. Dacuna, G.F. Burkhard, J.A. Bartelt, A. Salleo, M.F. Toney, M.D. McGehee, Adv. Energy Mater. **1**, 954 (2011).
22. X.H. Lu, H. Hlaing, D.S. Germack, J. Peet, W.H. Jo, D. Andrienko, K. Kremer, B.M. Ocko, Nat. Commun. **3**, 795 (2012).
23. M. Tong, S. Cho, J.T. Rogers, K. Schmidt, B.B.Y. Hsu, D. Moses, R.C. Coffin, E.J. Kramer, G.C. Bazan, A.J. Heeger, Adv. Funct. Mater. **20**, 3959 (2010).
24. J. Wang, M.J. Bedzyk, M. Caffrey, Science **258**, 775 (1992).
25. A.T. Yiu, P.M. Beaujuge, O.P. Lee, C.H. Woo, M.F. Toney, J.M.J. Fréchet, J. Am. Chem. Soc. **134**, 2180 (2012).
26. L.G. Parratt, Phys. Rev. **95**, 359 (1954).
27. M. Birkholz, P.F. Fewster, C. Genzel, *Thin film analysis by X-ray scattering* (Wiley-VCH, Weinheim, 2006).
28. E. Hecht, *Optics* (Addison-Wesley, 2002).